Journal of Alloys and Compounds 613 (2014) 344–350

Contents lists available at ScienceDirect

Journal of Alloys and Compounds

journal homepage: www.elsevier.com/locate/jalcom

Antiferromagnetism in $EuPdGe_3$

Mohammed A. Albedah [a], Khalid Al-Qadi [a,b], Zbigniew M. Stadnik [a,*], Janusz Przewoźnik [c]

[a] Department of Physics, University of Ottawa, Ottawa, Ontario K1N 6N5, Canada
[b] Department of Mathematics, Statistics and Physics, Qatar University, P.O. Box 2713, Doha, Qatar
[c] Solid State Physics Department, Faculty of Physics and Applied Computer Science, AGH University of Science and Technology, 30-059 Kraków, Poland

ARTICLE INFO

Article history:
Received 8 May 2014
Accepted 18 May 2014
Available online 2 June 2014

Keywords:
Antiferromagnet
^{151}Eu Mössbauer spectroscopy
$EuPdGe_3$

ABSTRACT

The results of X-ray diffraction, magnetic susceptibility and magnetization, and ^{151}Eu Mössbauer spectroscopy measurements of polycrystalline $EuPdGe_3$ are reported. $EuPdGe_3$ crystallizes in the $BaNiSn_3$-type tetragonal structure (space group $I4mm$) with the lattice constants $a = 4.4457(1)$ Å and $c = 10.1703(2)$ Å. The results are consistent with $EuPdGe_3$ being an antiferromagnet with the Néel temperature $T_N = 12.16(1)$ K and with the Eu spins $S = 7/2$ in the ab plane. The temperature dependence of the magnetic susceptibility above T_N follows the modified Curie-Weiss law with the effective magnetic moment of 7.82(1) μ_B per Eu atom and the paramagnetic Curie temperature of −5.3(1) K indicative of dominant antiferromagnetic interactions. The $M(H)$ isotherms for temperatures approaching T_N from above are indicative of dynamical short-range antiferromagnetic ordering in the sample. The temperature dependence of the hyperfine magnetic field follows a $S = 7/2$ Brillouin function. The principal component of the electric field gradient tensor is shown to increase with decreasing temperature and is well described by a $T^{3/2}$ power-law relation. The Debye temperature of $EuPdGe_3$ determined from the Mössbauer data is 199(2) K.

1. Introduction

There are more than 100 ternary compounds of the general chemical formula XYZ_3 that crystallize in different crystal structure types [1,2]. The largest number of XYZ_3 compounds crystallizes in the $BaNiSn_3$-type crystal structure [3], which belongs to the tetragonal space group $I4mm$ (No. 107). Among the $BaNiSn_3$-type compounds, the most intensively studied are those exhibiting superconductivity, heavy-fermion or Kondo lattice characteristics: $LaIrSi_3$ [4–8], $LaRhSi_3$ [5–7,10–13], $LaPdSi_3$ [14,15], $LaPtSi_3$ [15], $CeIrSi_3$ [7,8,16–21,9,22–33], $CeRhSi_3$ [7,16,11,17,18,21,34–49], $CeCoSi_3$ [6,21,50–57], $CeIrGe_3$ [16,21,9,57–62], $CeRhGe_3$ [16,21,60,58,63], $CeCoGe_3$ [58,57,64–72], $CeFeGe_3$ [73–75], $BaPtSi_3$ [76,77], $CaYSi_3$ (Y = Ir, Pt) [78], $SrYGe_3$ (Y = Pd, Pt) [77] and $SrAuSi_3$ [79]. Other compounds of the $BaNiSn_3$ structure type, such as $CeCuZ_3$ (Z = Al, Ga) [80], $XIrSi_3$ (X = Gd, Tb, Dy) [81,82], $GdCoSi_3$ [54,83], $GdYGa_3$ (Y = Ni, Cu) [83], $GdCuAl_3$ [83], $XCoGe_3$ (X = Pr, Nd) [84], $EuPtZ_3$ (Z = Si, Ge) [85,86], $XPdGe_3$ (X = La, Eu) [87,88], $EuNiGe_3$ [90,89] and $LaOsSi_3$ [91], are also reported and studied for their interesting physical properties. The presence of a very wide range of elements in the selected $BaNiSn_3$-type compounds indicated above point to the possibility of discovering new isostructural compounds of this type.

In this paper, we report on the synthesis and the results of crystallographic, magnetic, and ^{151}Eu Mössbauer spectroscopy investigations of a polycrystalline $EuPdGe_3$ compound. We demonstrate that this compound exhibits a long-range antiferromagnetic order below $T_N = 12.16(1)$ K with the Eu magnetic moments lying in the ab plane. We provide evidence for the presence of short-range antiferromagnetic correlations above T_N. We show that magnetic and Mössbauer data are consistent with the Eu atoms having spin 7/2. We find that the Debye temperature of $EuPdGe_3$ is 199(2) K.

2. Experimental methods

The polycrystalline sample of $EuPdGe_3$ was prepared using the constituent elements of Eu (purity 99.9%), Pd (purity 99.99%), and Ge (purity 99.999%) in stoichiometric ratio. Appropriate amounts of these elements were weld sealed under a purified argon atmosphere into a tantalum container. The container in turn was held within an evacuated fused silica jacket to avoid its air oxidation. The mixture was melted at 1050 °C for 4 h, followed by annealing at 600 °C for 190 h, and then quenching into cold water.

X-ray diffraction measurements were performed at 298 K in Bragg–Brentano geometry on the PANanalytical X'Pert scanning diffractometer using Cu Kα radiation in the 2θ range 15–111.5° in steps of 0.02°. The $K\beta$ line was eliminated by using a Kevex PSi2 Peltier-cooled solid-state Si detector.

* Corresponding author.
E-mail address: stadnik@uottawa.ca (Z.M. Stadnik).

http://dx.doi.org/10.1016/j.jallcom.2014.05.115
0925-8388/

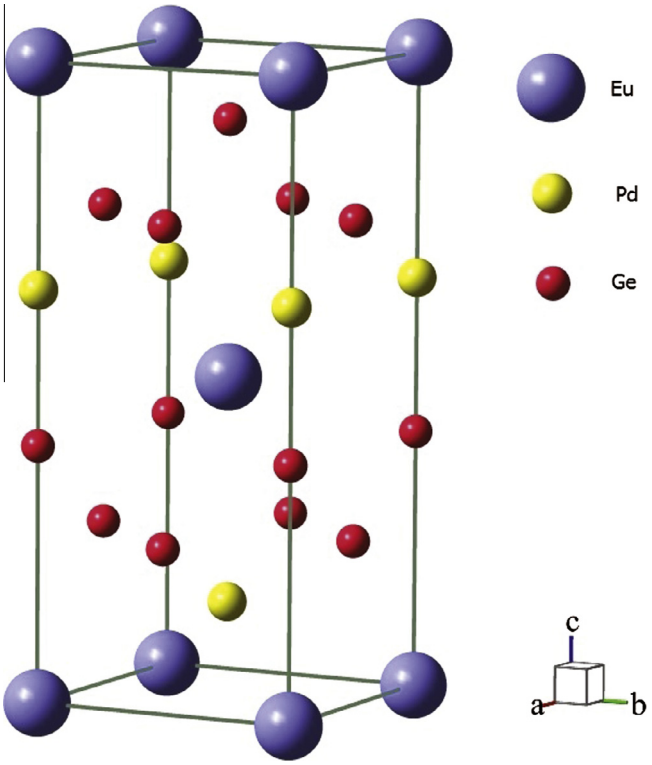

Fig. 1. The unit cell of the $EuPdGe_3$ compound.

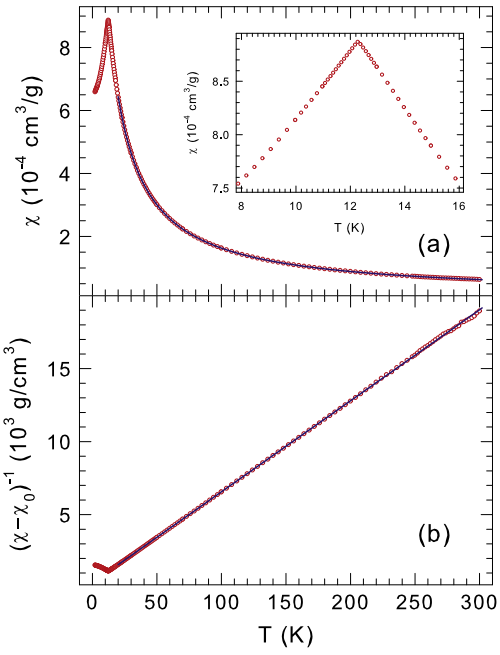

Fig. 3. (a) The temperature dependence of the magnetic susceptibility of $EuPdGe_3$, measured in an external magnetic field of 1000 Oe. The solid line is the fit to Eq. (1) in the temperature range 50–300 K, as explained in the text. The inset shows the magnetic susceptibility data in the low-temperature range. (b) The inverse magnetic susceptibility corrected for the contribution χ_0, $(\chi - \chi_0)^{-1}$ versus temperature T. The solid line is the fit to Eq. (1).

Table 1
Atomic positions for the tetragonal $EuPdGe_3$ obtained through Rietveld analysis.

Atom	Site	Point symmetry (mm)	Occupancy	x	y	z
Eu	2*a*	4	1.0	0	0	0
Pd	2*a*	4	1.0	0	0	0.645(2)
Ge	4*b*	2	1.0	0	$\frac{1}{2}$	0.257(2)
Ge	2*a*	4	1.0	0	0	0.403(2)

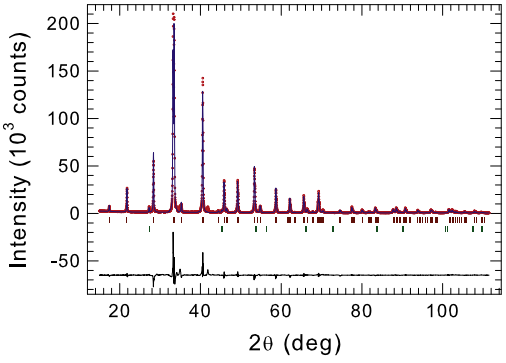

Fig. 2. The X-ray diffraction spectrum of the compound $EuPdGe_3$ at 298 K. The experimental data are denoted by open circles, while the line through the circles represents the results of the Rietveld refinement. The upper set of vertical bars represents the Bragg peak positions corresponding to the $EuPdGe_3$ phase, while the lower set refers to the positions of the impurity phase of Ge (space group $Fd\bar{3}m$). The lower solid line represents the difference curve between experimental and calculated spectra.

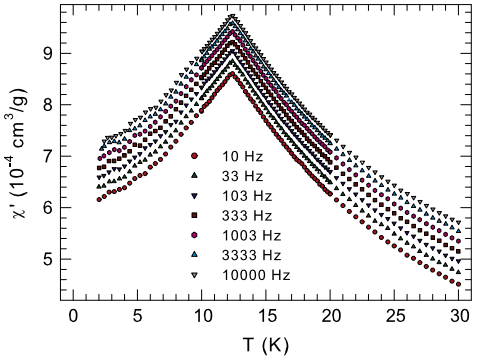

Fig. 4. Temperature dependence of the in-phase component χ' of the ac magnetic susceptibility of $EuPdGe_3$ for different applied frequencies from 10 to 10,000 Hz. As all these $\chi'(T)$ curves overlap, they are shifted upward with respect to each other by 2×10^{-5} cm^3/g.

The dc magnetization was measured in the temperature range 2–300 K and in magnetic fields up to 90 kOe using the vibrating sample magnetometer (VSM) option of the Quantum Design physical property measurement system (PPMS). The dc magnetic susceptibility was measured using PPMS in magnetic fields of 100 and 1000 Oe in the temperature range of 2–300 K. The ac magnetic susceptibility data were collected using PPMS between 2.0 and 30 K in a 10 Oe ac magnetic field and zero external dc magnetic field for frequencies varying from 10 Hz to 10 kHz.

The ^{151}Eu Mössbauer measurements were conducted using a standard, constant acceleration Mössbauer spectrometer operating in sine mode and a $^{151}Sm(SmF_3)$ source at room temperature. The 21.5 keV γ-rays were detected with a proportional counter. The spectrometer was calibrated with a Michelson interferometer [92], and the spectra were folded. The Mössbauer absorber consisted of a mixture of powder $EuPdGe_3$ and boron nitride, which was pressed into a pellet that was put into an Al disk container of thickness 0.008 mm to ensure a uniform temperature over the whole sample. The surface density of the Mössbauer absorber was 28.5 mg/cm^2. This corresponds to an effective thickness parameter [93] $T = 4.1 f_a$, where f_a is the Debye–Waller factor of the absorber. Since $T > 1$, the resonance line shape of the Mössbauer spectra was described using a transmission integral formula [94].

The Mössbauer source $^{151}Sm(SmF_3)$ used is not a monochromatic source as ^{151}Sm nuclei are located in the SmF_3 matrix at a site of noncubic symmetry. By measuring the ^{151}Eu Mössbauer spectra of a cubic EuSe compound we determined that the electric quadrupole coupling constant [93] eQ_gV_{zz} (here e is the proton charge, $Q_g = 0.903$ b (Ref. [95]) is the ground-state electric quadrupole moment of the ^{151}Eu nucleus, and V_{zz} is the principal component of the electric field gradient (EFG)

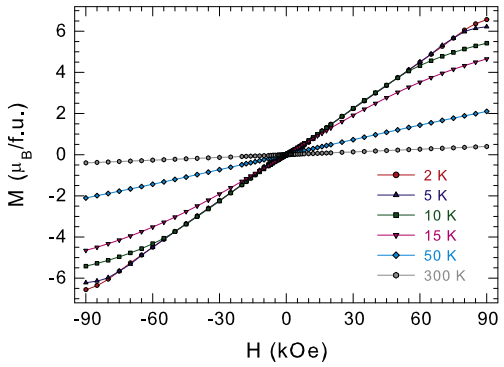

Fig. 5. Magnetization M versus applied magnetic field H isotherms of $EuPdGe_3$ measured at the indicated temperatures.

tensor) in our source is −3.69(13) mm/s, which is close to the value of −3.6 mm/s found in Ref. [96]. The precise shape of the source emission line was taken into account in the fits of the ^{151}Eu Mössbauer spectra. The isomer shift δ of the ^{151}Eu Mössbauer spectra is given here relative to the $^{151}Sm(SmF_3)$ source at room temperature.

3. Experimental results and discussion

3.1. Structural characterization

The ternary compound $EuPdGe_3$ crystallizes in the $BaNiSn_3$-type crystal structure with the tetragonal space group *I4mm* (No. 107) [97]. There are two formula units of $EuPdGe_3$ per unit cell. The crystal structure of $EuPdGe_3$ is shown in Fig. 1, with the crystallographic data for the Eu, Pd, and Ge sites listed in Table 1.

The room-temperature X-ray diffraction pattern of $EuPdGe_3$ is shown in Fig. 2. A Rietveld refinement [98] of the spectrum in Fig. 2 yields the lattice constants $a = 4.4457(1)$ Å and $c = 10.1703(2)$ Å. The values of these lattice parameters compare well with the corresponding values reported earlier [88,97]. As determined from the Rietveld refinement (Fig. 2), the $EuPdGe_3$ specimen contains a second phase of Ge (space group $Fd\bar{3}m$) in the amount of 1.0(2) wt%.

3.2. Magnetic measurements

The temperature dependence of the magnetic susceptibility χ of $EuPdGe_3$ measured in an applied magnetic field of 1000 Oe is

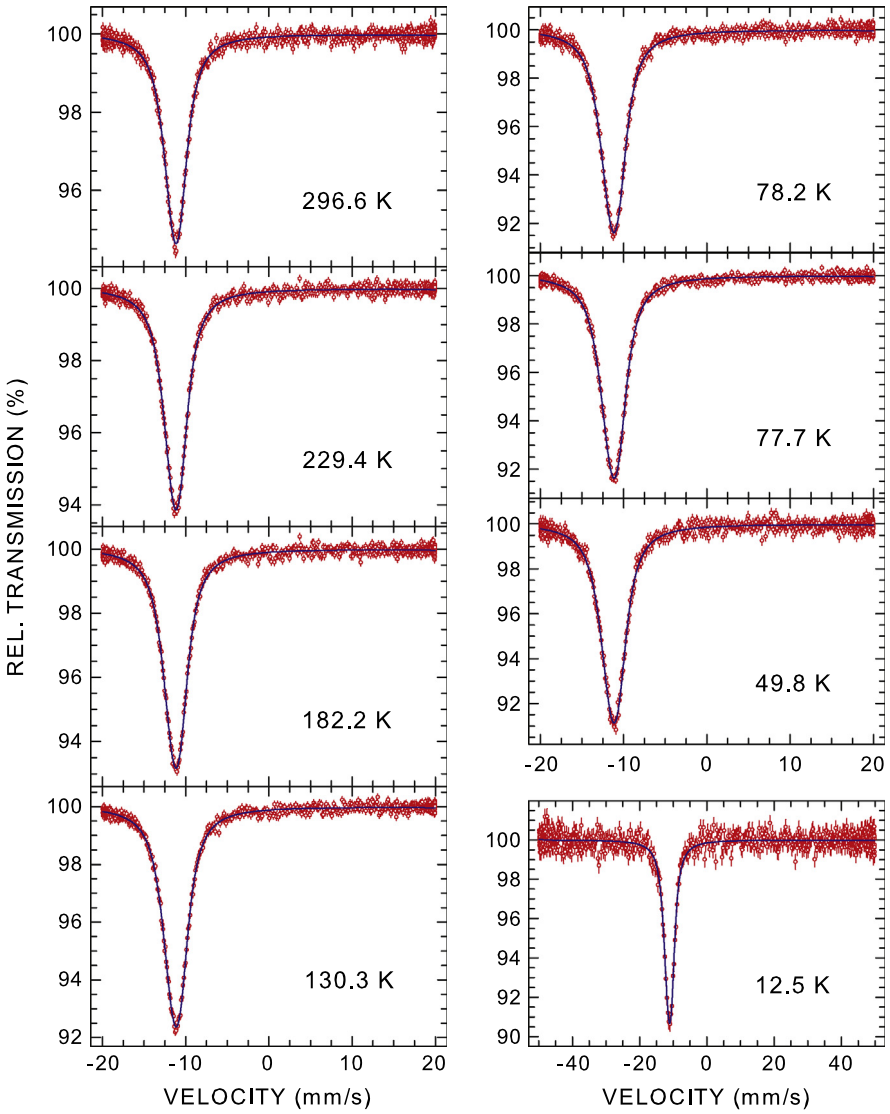

Fig. 6. ^{151}Eu Mössbauer spectra of $EuPdGe_3$ obtained at the indicated temperatures, fitted (solid lines) with an electric quadrupole hyperfine interaction, as described in the text. The zero-velocity origin is relative to the source.

shown in Fig. 3(a) (the identical $\chi(T)$ data were also obtained in an applied magnetic field of 100 Oe). The sharp peak at $T_N = 12.27(10)$ K in the $\chi(T)$ data is indicative of antiferromagnetic ordering occurring at this temperature.

The $\chi(T)$ data above 50 K (Fig. 3(a)) could be fitted to a modified Curie–Weiss law

$$\chi = \chi_0 + \frac{C}{T - \Theta_p}, \quad (1)$$

where χ_0 is the temperature-independent term that includes contributions from Pauli and Van Vleck paramagnetism as well as core and Landau diamagnetism, C is the Curie constant, and Θ_p is the paramagnetic Curie temperature. The Curie constant can be expressed as $C = \frac{N\mu_{eff}^2}{3k_B}$, where N is the number of Eu ions per formula unit, μ_{eff} is the effective magnetic moment, and k_B is the Boltzmann constant. Fig. 3(b) shows the inverse magnetic susceptibility corrected for the contribution χ_0 as $(\chi - \chi_0)^{-1}$ versus temperature; the validity of the modified Curie–Weiss law is evident. The values of χ_0, C, and Θ_p obtained from the fit are, respectively, $1.06(1) \times 10^{-5}$ cm^3/g, $16.04(3) \times 10^{-3}$ cm^3 K/g, and $-5.3(1)$ K. The value of C corresponds to $\mu_{eff} = 7.82(1)\ \mu_B$ per Eu atom.

For a free Eu^{2+} ion (electronic configuration $^8S_{7/2}$), the theoretical value of $\mu_{eff}^{th} = g\mu_B\sqrt{J(J+1)}$ is 7.94 μ_B [99]. The fact that the experimental value $\mu_{eff} = 7.82(1)\ \mu_B$ is close to the theoretical value of 7.94 μ_B confirms that the magnetic moment is localized on the divalent Eu ions. The negative value of Θ_p indicates the predominantly antiferromagnetic interaction between the Eu^{2+} magnetic moments.

Although the presence of a sharp peak in the $\chi(T)$ data is a necessary condition for the occurrence of antiferromagnetism, it is not a sufficient condition since a sharp peak in $\chi(T)$ is also observed for spin-glass compounds [100,101]. We therefore measured the temperature dependence of the in-phase component χ' of the ac magnetic susceptibility of $EuPdGe_3$ for selected frequencies between 10 and 10,000 Hz (Fig. 4). It is clear that the temperature of the maximum in $\chi'(T)$ curves does not depend on the frequency of the applied ac magnetic field, in contrast to its frequency dependence observed for spin glasses [100,101]. This confirms that the studied compound is an antiferromagnet.

The magnetization M versus applied magnetic field H isotherms of $EuPdGe_3$ at six temperatures between 2 and 300 K are shown in Fig. 5. It is seen from Fig. 5 that at 300 and 50 K the M exhibits a linear H dependence. However, the $M(H)$ curve for $T = 15$ K, i.e. slightly above T_N, has a downward curvature. This downward curvature is most probably due to dynamical short-range antiferromagnetic ordering in the sample on approaching T_N from above [90]. The presence of such a downward curvature in the $M(H)$ isotherms below T_N at $T = 2$, 5 and 10 K (Fig. 5) can be explained as being caused by a series of field-induced first-order spin-flop transitions where the ordered magnetic moments flop to a perpendicular orientation with respect the applied field [90]. It is a series of field-induced first-order spin-flop transitions occurring at increasing magnetic fields, rather than one first-order spin-flop transition in a single crystal occurring at a single magnetic field along the easy axis, because of the random orientation of the crystallites in the polycrystalline sample [90].

The maximum observed magnetization of 6.56 μ_B/Eu at $T = 2$ K and $H = 90$ kOe (Fig. 5) is rather close to the saturation magnetization ($M_{sat} = gS\mu_B$) of 7 μ_B/Eu expected for the free Eu^{2+} ion with $S = 5/2$ and $g = 2$. Within the mean-field theory, the critical field H_c at which M reaches M_{sat} with increasing H is equal to $M_{sat}/\chi(T_N)$. By taking the $\chi(T_N)$ value from Fig. 3, one obtains $H_c = 93$ kOe. This is close to the value of ~100 kOe estimated from an extrapolation of the $T = 2$ K isotherm (Fig. 5) to the value $M_{sat} = 7\mu_B$.

3.3. Mössbauer spectroscopy

The ^{151}Eu Mössbauer spectra of $EuPdGe_3$ recorded at temperatures at which no magnetic dipole hyperfine interaction [93] is present are shown in Fig. 6. These spectra are in a form of a broadened single line. The Eu atoms in $EuPdGe_3$ are located at the 2*a* site with the point symmetry 4/mm (Table 1), which ensures a non-zero, axially symmetric (the asymmetry parameter $\eta = 0$) EFG tensor at this site, and hence a non-zero electric quadrupole hyperfine interaction [93]. The spectra in Fig. 6 thus result from a pure electric quadrupole hyperfine interaction [102]. They were analyzed by means of a least-squares fitting procedure which entailed calculations of the positions and relative intensities of the absorption lines by numerical diagonalization of the full hyperfine interaction Hamiltonian [93]. The fit of the 296.6 K Mössbauer spectrum yields $eQ_gV_{zz} = 3.65(23)$ mm/s and $\delta = -11.23(1)$ mm/s. The value of δ proves that Eu is divalent in the studied compound [102].

The principal component of the EFG tensor V_{zz} derived from the fits of the spectra in Fig. 6 clearly increases with decreasing temperature [Fig. 7(a)]. In the traditional [103], i.e., not based on a first-principles method [104], interpretation of V_{zz} one uses the formula

$$V_{zz} = (1 - \gamma_\infty)V_{zz}^{ext} + (1 - R)V_{zz}^{local}, \quad (2)$$

where V_{zz}^{ext} is a contribution due to external (point) charges, V_{zz}^{local} is a contribution due to local charges (caused by valence and conduction electrons near the probe site), γ_∞ and R are, respectively, Steinheimer antishielding and shielding factors that account for the amplification or attenuation of V_{zz} resulting from the deformation of closed shells induced by V_{zz}^{ext} and V_{zz}^{local}, respectively. For Eu^{2+} ions with the $^8S_{7/2}$ ground state, the V_{zz}^{local} contribution is negligible and thus any V_{zz} must arise from the V_{zz}^{ext} contribution [105].

An increase of V_{zz} with decreasing temperature found here [Fig. 7(a)], was also observed in many other crystalline, amorphous, and quasicrystalline compounds [103,106–109]. Although

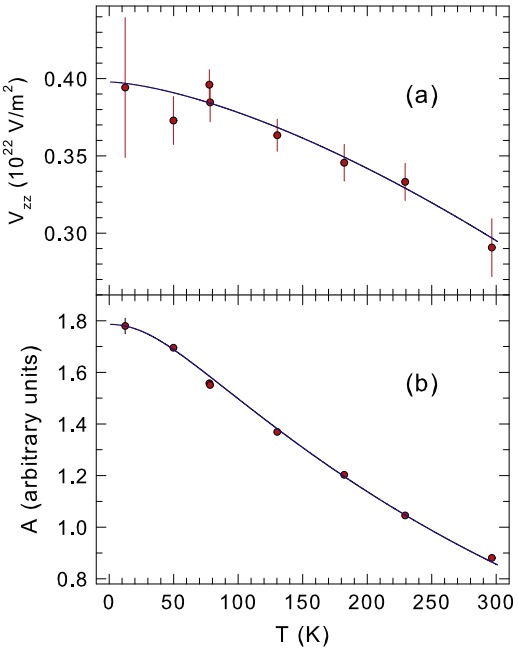

Fig. 7. Temperature dependence of (a) the principal component of the electric field gradient tensor V_{zz} and (b) the absorption spectral area A derived from the fits of the spectra in Fig. 6. The solid lines are the fits to Eq. (3) in (a) and to Eq. (4) in (b), as explained in the text.

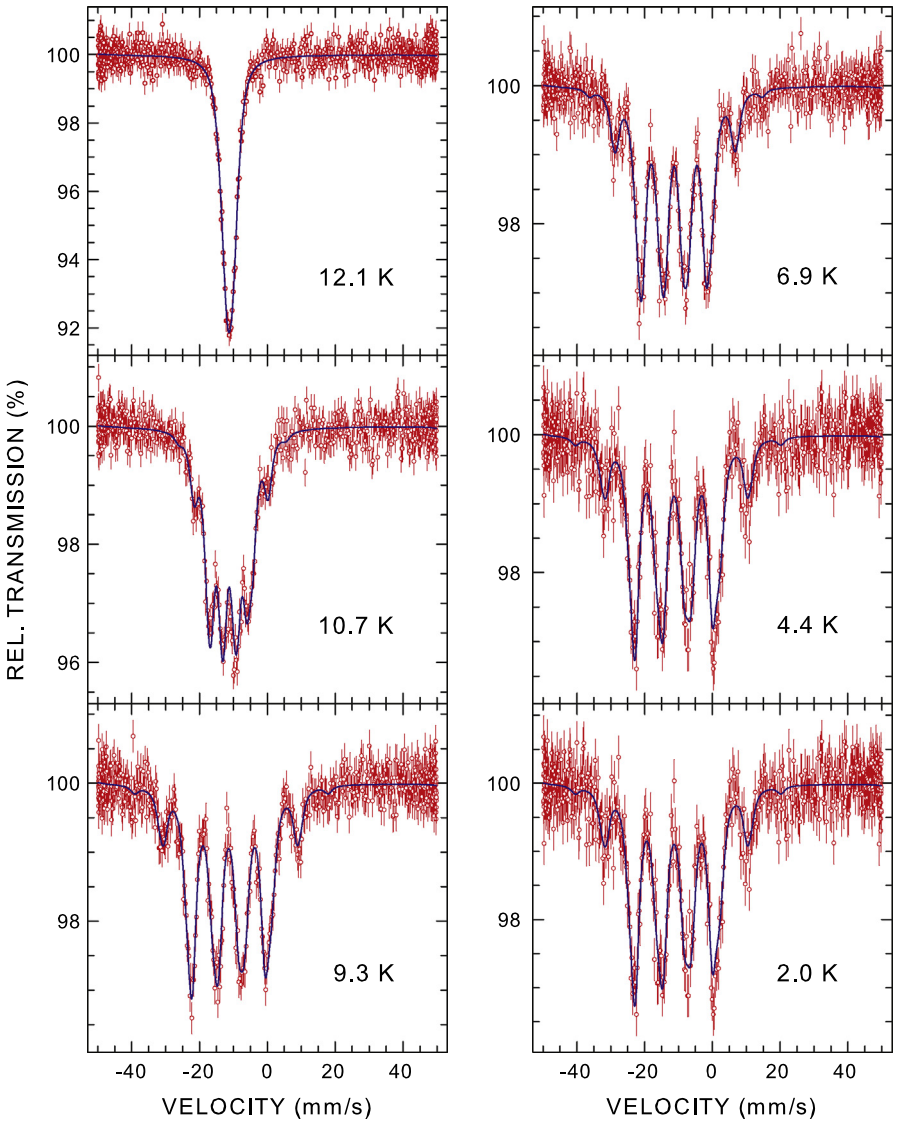

Fig. 8. ^{151}Eu Mössbauer spectra of $EuPdGe_3$ obtained at the indicated temperatures, fitted (solid lines) with combined magnetic dipole and electric quadrupole hyperfine interactions, as described in the text. The zero-velocity origin is relative to the source.

its mechanism is not well understood, it is surprisingly well described by the empirical relation [103]

$$V_{zz}(T) = V_{zz}(0)\left(1 - BT^{3/2}\right), \tag{3}$$

where $V_{zz}(0)$ is the value of V_{zz} at 0 K and B is a constant. The fit of the $V_{zz}(T)$ data [Fig. 7(a)] to Eq. (3) yields $V_{zz}(0) = 0.398(6) \times 10^{22}$ V/m^2 and $B = 4.97(70) \times 10^{-5}$ K$^{-3/2}$. We note that our value of $V_{zz}(0) = 0.398(6) \times 10^{22}$ V/m^2 is almost identical to the value of $V_{zz}(4.2\ \mathrm{K}) = 0.39 \times 10^{22}$ V/m^2 at the Gd site in the isostructural $GdCoSi_3$ as determined from ^{155}Gd Mössbauer spectroscopy [83]. The value of B found here is similar to that found for other systems [103,107].

Fig. 7(b) displays the temperature dependence of the absorption spectral area A derived from the fits of the Mössbauer spectra in Fig. 6. This area is proportional to the absorber Debye–Waller factor f_a given [93] by

$$f_a(T) = \exp\left\{-\frac{3}{4}\frac{E_\gamma^2}{Mc^2 k_B \Theta_D}\left[1 + 4\left(\frac{T}{\Theta_D}\right)^2 \int_0^{\Theta_D/T} \frac{x\,dx}{e^x - 1}\right]\right\}, \tag{4}$$

where M is the mass of the Mössbauer nucleus, c is the speed of light, E_γ is the energy of the Mössbauer transition, and Θ_D is the Debye temperature. The fit of the $A(T)$ data [Fig. 7(b)] to Eq. (4) gives $\Theta_D = 199(2)$ K. The value of Θ_D found here should be compared with the value of 268(2) K derived from the specific heat data for the isostructural $EuNiGe_3$ [90].

The ^{151}Eu Mössbauer spectra of $EuPdGe_3$ measured at temperatures at which both magnetic dipole and electric quadrupole hyperfine interactions are present are shown in (Fig. 8). The fit of the 2.0 K Mössbauer spectrum yields the following values of the hyperfine parameters: $\delta = -11.15(5)$ mm/s, the hyperfine magnetic field $H_{hf} = 293.4(1.3)$ kOe, $eQ_gV_{zz} = 4.98(87)$ mm/s, and the angle between the direction of H_{hf} and the V_{zz}-axis $\theta = 92(5)^\circ$. As the principal axis of the EFG tensor (V_{zz}-axis) is along the tetragonal c-axis, the value $\theta = 92(5)^\circ$ implies that the Eu magnetic moments in $EuPdGe_3$ must lie in the ab plane. We note here that it was suggested [90] that the Eu magnetic moments are also aligned in the ab plane in the isostructural $EuNiGe_3$. Similarly, in the isostructural $GdCoSi_3$ the Gd magnetic moments were shown with ^{155}Gd Mössbauer spectroscopy to be perpendicular to the crystallographic c axis [83].

The temperature dependence of H_{hf} determined from the fits to the Mössbauer spectra in Fig. 8 is shown in Fig. 9. It is usually assumed that the temperature variation of H_{hf} in an

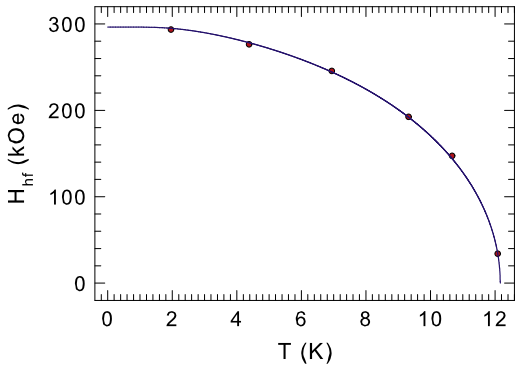

Fig. 9. Temperature dependence of the hyperfine magnetic field H_{hf} determined from the fits of the spectra in Fig. 8. The solid line is the fit to Eq. (5), as explained in the text.

antiferromagnet can be reasonably explained in term of the molecular field model, assuming that H_{hf} is proportional to the sublattice magnetization. In terms of this model, $H_{hf}(T)$ can be expressed as

$$H_{hf}(T) = H_{hf}(0)B_J(x), \tag{5}$$

where $H_{hf}(0)$ is the saturation hyperfine magnetic field, $B_J(x)$ is the Brllouin function defined as

$$B_J(x) = \frac{2J+1}{2J}\coth\left(\frac{2J+1}{2J}x\right) - \frac{1}{2J}\coth\left(\frac{x}{2J}\right) \tag{6}$$

and

$$x = \frac{3J}{J+1}\frac{H_{hf}(T)}{H_{hf}(0)}\frac{T_N}{T}. \tag{7}$$

The fit of the $H_{hf}(T)$ data (Fig. 9) to Eq. (5) with $J = S = 7/2$ yields $H_{hf}(0) = 296.4(1.1)$ kOe and $T_N = 12.16(1)$ K. We believe that the value of T_N determined here is more precise than that determined from the position of the peak in the $\chi(T)$ data (Fig. 3).

In principle, one could attempt to estimate the saturation magnetic moment of Eu in the studied compound from the value of $H_{hf}(0)$ found here, based on the expected proportionality between the latter and the former. The hyperfine magnetic field at the ^{151}Eu nucleus in a metallic system can be written as the sum of three contributions [110]

$$H_{hf} = H_{core} + H_{cep} + H_n, \tag{8}$$

where H_{core} is the core-polarization field, H_{cep} is the contribution of the valence and conduction band electrons, and H_n includes all contributions from neighboring magnetic moments. It is only the H_{core} contribution that is truly proportional to the Eu magnetic moment. However, since all these three contributions are approximately of a similar magnitude [102], one is unable to determine the magnitude of the Eu magnetic moment from the measured value of H_{hf}.

4. Conclusions

We have reported the results of X-ray diffraction, magnetic susceptibility and magnetization, and ^{151}Eu Mössbauer spectroscopy measurements of the $EuPdGe_3$ compound. The studied compound crystallizes in the $BaNiSn_3$-type crystal structure with the lattice constants $a = 4.4457(1)$ Å and $c = 10.1703(2)$ Å. The high-temperature $\chi(T)$ data follow the modified Curie–Weiss law with a Curie constant consistent with Eu^{2+} spins $S = 7/2$ and Weiss temperature $\Theta_p = -5.3(1)$ K indicative of dominant antiferromagnetic interactions. We find that $EuPdGe_3$ is an antiferromagnet with the Néel temperature $T_N = 12.16(1)$ K and the Eu ordered magnetic moments in the *ab* plane. The temperature dependence of the hyperfine magnetic field is well described by a $S = 7/2$ Brillouin function. Evidence of dynamical short-range antiferromagnetic ordering in the sample is observed in the $M(H)$ curves on approaching T_N from above. The shape of the $M(H)$ isotherms at temperatures below T_N is indicative of a series of field-induced first-order spin-flop transitions where the ordered magnetic moments flop to a perpendicular orientation with respect the the applied field. The principal component of the electric field gradient tensor increases with decreasing temperature and is well described by a $T^{3/2}$ power-law relation. The Debye temperature of $EuPdGe_3$ is found to be 199(2) K.

Acknowledgment

This work was supported by the Natural Sciences and Engineering Research Council of Canada.

References

[1] PDF-4+ 2013 Database, The International Centre for Diffraction Data, Newtown Square, PA 19073-3273, U.S.A.
[2] The Inorganic Crystal Structure Database, Fachinformationszentrum Karlsruhe GmbH, Eggenstein-Leopoldshafen, Germany.
[3] W. Dörrscheidt, H. Schäfer, J. Less-Common Met. 58 (1978) 209.
[4] N. Engel, H.F. Braun, E. Parthé, J. Less-Common Met. 95 (1983) 309.
[5] P. Lejay, I. Higashi, B. Chevalier, J. Etourneau, P. Hagenmuller, Mater. Res. Bull. 19 (1984) 115.
[6] P. Haen, P. Lejay, B. Chevalier, J. Etourneau, M. Sera, J. Less-Common Met. 110 (1985) 321.
[7] M.B.T. Tchokonté, P.de V. du Plessis, A.M. Strydom, Solid State Commun. 117 (2001) 321.
[8] Y. Okuda, Y. Miyauchi, Y. Ida, Y. Takeda, C. Tonohiro, Y. Oduchi, T. Yamada, N.D. Dung, T.D. Matsuda, Y. Haga, T. Takeuchi, M. Hagiwara, K. Kindo, H. Harima, K. Sugiyama, R. Settai, Y. Ōnuki, J. Phys. Soc. Jpn. 76 (2007) 044708.
[9] Y. Okuda, I. Sugitani, H. Shishido, T. Yamada, A. Thamizhavel, E. Yamamoto, T.D. Matsuda, Y. Haga, T. Takeuchi, R. Settai, Y. Ōnuki, J. Magn. Magn. Mater. 310 (2007) 563.
[10] N. Kimura, Y. Umeda, T. Asai, T. Terashima, H. Aoki, Physica B 294–295 (2001) 280.
[11] T. Terashima, M. Kimata, S. Uji, T. Sugawara, N. Kimura, H. Aoki, H. Harima, Phys. Rev. B 78 (2008) 205107.
[12] V.K. Anand, A.D. Hillier, D.T. Adroja, A.M. Strydom, H. Michor, K.A. McEwen, B.D. Rainford, Phys. Rev. B 83 (2011) 064522.
[13] N. Kurita, C.F. Miclea, C. Putzke, G. Seyfarth, C. Capan, A. Bianchi, Z. Fisk, J.D. Thompson, R. Movshovich, J. Phys. Conf. Ser. 273 (2011) 012077.
[14] J. Kitagawa, Y. Muro, N. Takeda, M. Ishikawa, J. Phys. Soc. Jpn. 66 (1997) 2163.
[15] M. Smidman, A.D. Hillier, D.T. Adroja, M.R. Lees, V.K. Anand, R.P. Singh, R.I. Smith, D.M. Paul, G. Balakrishnan, arXiv:1402.4961v1.
[16] Y. Muro, D. Eom, N. Takeda, M. Ishikawa, J. Phys. Soc. Jpn. 67 (1998) 3601.
[17] Y. Muro, D.H. Eom, N. Takeda, M. Ishikawa, K. Kanai, M. Watanabe, S. Shin, Physica B 259–261 (1999) 1114.
[18] A. Krimmel, M. Reehuis, A. Loidl, Appl. Phys. A 74 (2002) S695.
[19] I. Sugitani, Y. Okuda, H. Shishido, T. Yamada, A. Thamizhavel, E. Yamamoto, T.D. Matsuda, Y. Haga, T. Takeuchi, R. Settai, Y. Ōnuki, J. Phys. Soc. Jpn. 75 (2006) 043703.
[20] R. Settai, T. Takeuchi, Y.Y. Ōnuki, J. Phys. Soc. Jpn. 77 (2007) 051003.
[21] T. Shimoda, Y. Okuda, Y. Takeda, Y. Iida, Y. Miyauchi, T. Kawai, T. Fujie, I. Sugitane, A. Thamizhavel, T.D. Matsuda, Y. Haga, T. Takeuchi, M. Nakashimad, R. Settai, Y.Y. Ōnuki, J. Magn. Magn. Mater. 310 (2007) 308.
[22] R. Settai, T.Y. Miyauchi, Takeuchi, F. Lévy, I. Sheikin, Y. Ōnuki, J. Phys. Soc. Jpn. 77 (2008) 073705.
[23] F. Tomioka, M. Hedo, I. Umehara, Y. Uwatoko, Y. Takano, Y. Okuda, R. Settai, Y. Ōnuki, J. Phys. Chem. Solids 69 (2008) 3199.
[24] H. Mukuda, T. Fujii, T. Ohara, A. Harada, M. Yashima, Y. Kitaoka, Y. Okuda, R. Settai, Y. Onuki, Phys. Rev. Lett. 100 (2008) 107003.
[25] Y. Ōnuki, H. Shishido, Y. Okuda, Y. Miyauchi, R. Settai, T. Takeuchi, T.D. Matsuda, N. Tateiwa, Y. Haga, H. Harima, Physica B 403 (2008) 963.
[26] N. Tateiwa, Y. Haga, S. Ikeda, T.D. Matsuda, E. Yamamoto, Y. Okuda, Y. Miyauchi, R. Settai, Y. Ōnuki, Physica B 403 (2008) 1156.
[27] T. Ohkochi, T. Toshimitsu, H. Yamagami, S. Fujimori, A. Yasui, Y. Takeda, T. Okane, Y. Saitoh, A. Fujimori, Y. Miyauchi, Y. Okuda, R. Settai, Y. Ōnuki, J. Phys. Soc. Jpn. 78 (2009) 084802.
[28] H. Mukuda, T. Ohara, M. Yashima, Y. Kitaoka, R. Settai, Y. Ōnuki, K.M. Itoh, E.E. Haller, Phys. Rev. Lett. 104 (2010) 017002.
[29] R. Settai, K. Katayama, D. Aoki, I. Sheikin, G. Knebel, J. Flouquet, Y. Ōnuki, J. Phys. Soc. Jpn. 80 (2011) 094703.
[30] N. Aso, M. Takahashi, H. Yoshizawa, H. Iida, N. Kimura, H. Aoki, J. Phys. Soc. Jpn. 80 (2011) 095004.
[31] Y. Takaesu, N. Aso, Y. Tamaki, M. Haedo, T. Nakama, K. Uchima, H. Iida, N. Kimura, H. Aoki, J. Phys. Soc. Jpn. 80 (2011) SA068.

[32] N. Aso, M. Takahashi, H. Yoshizawa, H. Iida, N. Kimura, H. Aoki, J. Phys. Conf. Ser. 400 (2012) 022003.
[33] Y. Ōnuki, R. Settai, Y. Miura, H. Tsutsumi, F. Honda, H. Harima, Phys. Status Solidi B 250 (2013) 583.
[34] N. Kimura, K. Ito, K. Saitoh, Y. Umeda, H. Aoki, T. Terashima, Phys. Rev. Lett. 95 (2005) 247004.
[35] N. Kimura, Y. Muro, H. Aoki, J. Phys. Soc. Jpn. 76 (2007) 051010.
[36] N. Aso, H. Miyano, H. Yoshizawa, N. Kimura, T. Komatsubara, H. Aoki, J. Magn. Magn. Mater. 310 (2007) 602.
[37] F. Tomioka, M. Hedo, I. Umehara, T. Ono, Y. Uwatoko, N. Kimura, S. Takayanagi, J. Magn. Magn. Mater. 310 (2007) 340.
[38] Y. Muro, M. Ishikawa, K. Hirota, Z. Hiroi, N. Takeda, N. Kimura, H. Aoki, J. Phys. Soc. Jpn. 76 (2007) 033707.
[39] T. Terashima, Y. Takahide, T. Matsumoto, S. Uji, N. Kimura, H. Aoki, H. Harima, Phys. Rev. B 76 (2007) 054507.
[40] I. Umehara, M. Hedo, F. Tomioka, Y. Uwatoko, J. Phys. Soc. Jpn. Suppl. A 76 (2007) 206.
[41] F. Tomioka, I. Emehara, T. Ono, M. Hedo, Y. Uwatoko, N. Kimura, Jpn. J. Appl. Phys. 46 (2007) 3090.
[42] T. Sugawara, N. Kimura, H. Aoki, F. Lévy, I. Sheikin, T. Terashima, J. Phys. Soc. Jpn. 79 (2010) 063701.
[43] T. Sugawara, N. Kimura, H. Aoki, T. Trashima, F. Lévy, I. Sheikin, J. Phys. Conf. Ser. 200 (2010) 012194.
[44] N. Kimura, T. Sugawara, H. Aoki, T. Terashima, Physica C 470 (2010) S529.
[45] T. Sugawara, N. Kimura, H. Aoki, J. Phys. Soc. Jpn. 80 (2011) SA067.
[46] N. Kimura, T. Sugawara, H. Aoki, J. Phys. Soc. Jpn. 80 (2011) SA019.
[47] T. Sugawara, H. Iida, H. Aoki, N. Kimura, J. Phys. Soc. Jpn. 81 (2012) 054711.
[48] N. Egetenmeyer, J.L. Gavilano, A. Maisuradze, S. Gerber, D.E. MacLaughlin, G. Seyfarth, D. Andreica, A. Desilets-Benoit, A.D. Bianchi, Ch. Baines, R. Khasanov, Z. Fisk, M. Kenzelmann, Phys. Rev. Lett. 108 (2012) 177204.
[49] H. Iida, T. Sugawara, H. Aoki, N. Kimura, Phys. Status Solidi B 250 (2013) 502.
[50] V.V. Nemoshkalenko, P.K. Nikolyuk, P.V. Gel, L.I. Nikolaev, V. Kh. Kasiyanenko, A.V. Khrushchak, B.P. Mamko, Phys. Status Solidi B 152 (1989) K55.
[51] Y. Iwamoto, K. Ueda, T. Kohara, Y. Yamada, Physica B 206–207 (1995) 276.
[52] D. Eom, M. Ishikawa, J. Kitagawa, N. Takeda, J. Phys. Soc. Jpn. 67 (1998) 2495.
[53] K. Kanai, T. Terashima, D.H. Eom, M. Ishikawa, S. Shin, Phys. Rev. B 60 (1999) 9900(R).
[54] J.B. Hong, J.W. Kim, K.E. Lee, N.A. Lee, K.H. Jang, J.-G. Park, Y.S. Kwon, J. Magn. Magn. Mater. 310 (2007) 292.
[55] H. Iida, Y. Kadota, M. Kogure, T. Sugawara, H. Aoki, N. Kimura, J. Phys. Soc. Jpn. 80 (2011) 083701.
[56] M. Smidman, R.P. Singh, M.R. Lees, D. M'k Paul, D.T. Adroja, G. Balakrishnan, J. Phys. Conf. Ser. 391 (2012) 012068.
[57] F. Honda, Y. Hirose, S. Yoshiuchi, S. Yasui, T. Takeuchi, I. Bonalde, K. Shimizu, R. Settai, Y. Ōnuki, J. Phys. Conf. Ser. 400 (2012) 022028.
[58] T. Kawai, M. Nakashima, Y. Okuda, H. Shishido, T. Shimoda, T.D. Matsuda, Y. Haga, T. Takeuchi, M. Hedo, Y. Uwatoko, R. Settai, Y. Ōnuki, J. Phys. Soc. Jpn. Suppl. A 76 (2007) 166.
[59] T. Kawai, H. Muranaka, M.-A. Measson, T. Shimoda, Y. Doi, T.D. Matsuda, Y. Haga, G. Knebel, G. Lapertot, D. Aoki, J. Flouquet, T. Takeuchi, R. Settai, Y. Ōnuki, J. Phys. Soc. Jpn. 77 (2008) 064716.
[60] S. Nishigori, S. Nagira, J. Phys. Conf. Ser. 150 (2009) 042143.
[61] F. Honda, I. Bonalde, S. Yoshiuchi, Y. Hirose, T. Nakamura, K. Shimizu, R. Settai, Y. Ōnuki, Physica C 470 (2010) S543.
[62] F. Honda, I. Bonalde, K. Shimizu, S. Yoshiuchi, Y. Hirose, T. Nakamura, R. Settai, Y. Ōnuki, Phys. Rev. B 81 (2010) 140507(R).
[63] A.D. Hillier, D.T. Adroja, P. Manuel, V.K. Anand, J.W. Taylor, K.A. McEwen, B.D. Rainford, M.M. Koza, Phys. Rev. B 85 (2012) 134405.
[64] V.K. Pecharsky, O.-B. Hyun, K.A. Gschneidner Jr., Phys. Rev. B 47 (1993) 11839.
[65] A. Das, A.K. Nigam, J. Phys.: Condens. Matter 12 (2000) 1315.
[66] A. Das, R.K. Kremer, R. Pöttgen, B. Ouladdiaf, Physica B 378–380 (2006) 837.
[67] A. Thamizhavel, H. Shishido, Y. Okuda, H. Harima, T.D. Matsuda, Y. Haga, R. Settai, Y. Ōnuki, J. Phys. Soc. Jpn. 75 (2006) 044711.
[68] R. Settai, Y. Okuda, I. Sugitani, Y. Ōnuki, T.D. Matsuda, Y. Haga, H. Harima, Int. J. Mod. Phys. B 21 (2007) 3238.
[69] G. Knebel, D. Aoki, G. Lapertot, B. Salce, J. Flouquet, T. Kawai, H. Muranaka, R. Settai, Y. Ōnuki, J. Phys. Soc. Jpn. 78 (2009) 074714.
[70] M.-A. Méasson, H. Muranaka, T.D. Matsuda, T. Kawai, Y. Haga, G. Knebel, D. Aoki, G. Lapertot, F. Honda, R. Settai, J.-P. Brison, J. Flouquet, K. Shimizu, Y. Onuki, Physica C 470 (2010) S536.
[71] I. Sheikin, P. Rodiere, R. Settai, Y. Ōnuki, J. Phys. Soc. Jpn. 80 (2011) SA020.
[72] M. Smidman, D.T. Adroja, A.D. Hillier, L.C. Chapon, J.W. Taylor, V.K. Anand, R.P. Singh, M.R. Lees, E.A. Goremychkin, M.M. Koza, V.V. Krishnamurthy, D.M. Paul, G. Balakrishnan, Phys. Rev. B 88 (2013) 134416.
[73] H. Yamamoto, H. Sawa, M. Ishikawa, Phys. Lett. A 196 (1994) 83.
[74] H. Yamamoto, M. Ishikawa, K. Hasegawa, J. Sakurai, Phys. Rev. B 52 (1995) 10136.
[75] S.L. Bud'ko, M.B. Fontes, E.M. Baggio-Saitovitch, J. Phys.: Condens. Matter 10 (1998) 8815.
[76] E. Bauer, R.T. Khan, H. Michor, E. Royanian, A. Grytsiv, N. Melnychenko-Koblyuk, P. Rogl, D. Reith, R. Podloucky, E.-W. Scheidt, W. Wolf, M. Marsman, Phys. Rev. B 80 (2009) 064504.
[77] K. Miliyanchuk, F. Kneidinger, C. Blaas-Schenner, D. Reith, R. Podloucky, P. Rogl, T. Khan, L. Salamakha, G. Hilscher, H. Michor, E. Bauer, A.D. Hillier, J. Phys. Conf. Ser. 273 (2011) 012078.
[78] G. Eguchi, D.C. Peets, M. Kriener, Y. Maeno, E. Nishibori, Y. Kumazawa, K. Banno, S. Maki, H. Sawa, Phys. Rev. B 83 (2011) 024512.
[79] M. Isobe, H. Yoshida, K. Kimoto, M. Arai, E. Takayama-Muromachi, Chem. Mater. 26 (2014) 2155.
[80] S.A.M. Mentink, N.M. Bos, B.J. van Rossum, G.J. Nieuwenhuys, J.A. Mydosh, K.H.J. Buschow, J. Appl. Phys. 73 (1993) 6625.
[81] J.P. Sanchez, K. Tomala, K. Łtka, J. Magn. Magn. Mater. 99 (1991) 95.
[82] W. Bażela, N. Stüsser, A. Szytuła, A. Zygmunt, J. Alloys Comp. 275–277 (1998) 578.
[83] F.M. Mulder, R.C. Thiel, K.H.J. Buschow, J. Alloys Comp. 216 (1994) 95.
[84] M.-a. M'easson, H. Muranaka, T. Kawai, Y. Ota, K. Sugiyama, M. Hagiwara, K. Kindo, T. Takeuchi, K. Shimizu, F. Honda, R. Settai, Y. Ōnuki, J. Phys. Soc. Jpn. 78 (2009) 124713.
[85] N. Kumar, S.K. Dhar, A. Thamizhavel, P. Bonville, P. Manfrinetti, Phys. Rev. B 81 (2010) 144414.
[86] N. Kumar, P.K. Das, R. Kulkarni, A. Thamizhavel, S.K. Dhar, P. Bonville, J. Phys.: Condens. Matter 24 (2012) 036005.
[87] R. Troć, R. Wawryk, A.V. Gribanov, J. Alloys Comp. 581 (2013) 659.
[88] D. Kaczorowski, B. Bela, Gladyshevskii, Solid State Commun. 152 (2012) 839.
[89] A. Maurya, P. Bonville, A. Thamizhavel, S.K. Dhar, J. Phys.: Condens. Matter 26 (2014) 216001.
[90] R.J. Goetsch, V.K. Anand, D.C. Johnston, Phys. Rev. B 87 (2013) 064406.
[91] X. Zhang, S.-S. Miao, P. Wang, P. Zheng, W.-L. Yin, J.-Y. Yao, H.-W. Jiang, H. Wang, Y.-G. Shi, Chin. Phys. B 22 (2013) 108103.
[92] B.F. Otterloo, Z.M. Stadnik, A.E.M. Swolfs, Rev. Sci. Instrum. 54 (1983) 1575.
[93] N.N. Greenwood, T.C. Gibb, Mössbauer Spectroscopy, Chapman and Hall, London, 1971;
P. Gütlich, E. Bill, A. Trautwein, Mössbauer Spectroscopy and Transition Metal Chemistry, Springer, Berlin, 2011.
[94] S. Margulies, J.R. Ehrman, Nucl. Instrum. Methods 12 (1961) 131;
G.K. Shenoy, J.M. Friedt, H. Maletta, S.L. Ruby, in: I.J. Gruverman, C.W. Seidel, D.K. Dieterly (Eds.), Mössbauer Effect Methodology, vol. 10, Plenum, New York, 1974, p. 277.
[95] Y. Tanaka, R.M. Steffen, E.B. Shera, W. Reuter, M.V. Hoehn, J.D. Zumbro, Phys. Rev. C 29 (1984) 1830.
[96] I. Nowik, I. Felner, Hyperfine Interact. 28 (1986) 959.
[97] PDF4+ 2013 Database, Card No. 04-005-7675.
[98] R.A. Young, The Rietveld Method, Oxford University Press, Oxford, 1993.
[99] N.W. Ashcroft, N.D. Mermin, Solid State Physics, Saunders, Philadelphia, 1976.
[100] P. Wang, Z.M. Stadnik, J. Żukrowski, B.K. Cho, J.Y. Kim, Phys. Rev. B 82 (2010) 134404.
[101] P. Wang, Z.M. Stadnik, J. Przewoźnik, J. Alloys Comp. 509 (2011) 3435.
[102] F. Grandjean, G.J. Long, in: G.J. Long, F. Grandjean (Eds.), Mössbauer Spectroscopy Applied to Inorganic Chemistry, vol. 3, Plenum, New York, 1989, p. 513.
[103] E.N. Kaufmann, R.J. Vianden, Rev. Mod. Phys. 51 (1979) 161. and references therein.
[104] P. Blaha, K. Schwarz, P. Herzig, Phys. Rev. Lett. 54 (1985) 1192.
[105] Z.M. Stadnik, G. Stroink, T. Arakawa, Phys. Rev. B 44 (1991) 12552. and references therein.
[106] A. Comment, J.-P. Ansermet, C.P. Slichter, H. Rho, C.S. Snow, S.L. Cooper, Phys. Rev. B 72 (2005) 014428.
[107] K. Al-Qadi, P. Wang, Z.M. Stadnik, J. Przewoźnik, Phys. Rev. B 79 (2009) 224202. and references therein.
[108] P. Wang, Z.M. Stadnik, J. Żukrowski, B.K. Cho, J.Y. Kim, Phys. Rev. B 82 (2010) 134404.
[109] P. Wang, Z.M. Stadnik, J. Żukrowski, B.K. Cho, J.Y. Kim, Solid State Commun. 150 (2010) 2168.
[110] I. Nowik, B.D. Dunlap, J.H. Wernick, Phys. Rev. B 8 (1973) 238.